doi: 10.17221/81/2017-VETMED

Imaging features of bilateral primary megaureter in a senior dog: a case report

H. Yoon, J. Kim, Y.M. Ha, K. Eom*

Department of Veterinary Medical Imaging, College of Veterinary Medicine, Konkuk University, Seoul, Republic of Korea

*Corresponding author: eomkd@konkuk.ac.kr

ABSTRACT: An 8-year-old dog weighing 45 kg presented with symmetric alopecia, diarrhoea and undescended testes with no associated urinary symptoms. Abdominal ultrasonography and computed tomographic excretory urography revealed extensive dilation and reduced peristalsis of both ureters, except for the distal parts, which showed normal insertion into the urinary bladder, and normal calibre without peristalsis. No abnormalities of the urinary bladder or urethra that may have caused obstruction were identified. A diagnosis of primary megaureter was made. This is the first known reported case of primary megaureter in a dog. To our knowledge, this is first known case report in the veterinary literature that describes the ultrasonographic features of primary megaureter.

Keywords: Alaskan malamute dog; canine; dilated ureter; renogram; sustentacular cell tumour

In human studies, a megaureter is defined as a ureter with a diameter of 7 mm or more (Kass 1992). However definitive criteria for defining the megaureter have not been established in animals. Megaureter can cause secondary urinary infection and reduced renal function (Gimpel et al. 2010), and it is categorised into primary megaureter due to anomalies of the ureter or vesicoureteral junction, and secondary megaureter due to congenital and acquired obstructive abnormalities of the bladder or urethra (Berrocal et al. 2002). The primary megaureter is an idiopathic megaureter that excludes obstructive and neurological problems of the urethra or urinary bladder and polyuria (Shokeir and Nijman 2000). Because primary megaureter is often accompanied by urinary tract infections, infection is not included in the diagnostic criteria of primary megaureter (Shokeir and Nijman 2000; Khoury and Bagli 2007).

In a human study, primary megaureter was classified as refluxing primary megaureter, obstructed primary megaureter or non-refluxing unobstructed primary megaureter (Smith et al. 1977). Refluxing primary megaureter mainly occurs because of abnormal maturation of the vesicoureteral junction (Berrocal et al. 2002), which weakens its valve-like function, resulting in reflux and ascending dissemination of bacteria (Gross and Lebowitz 1981; Berrocal et al. 2002). Obstructed primary megaureter is related to a short and aperistaltic distal ureteral section (0.5–4 cm) with normal calibre connected to the vesicoureteral junction. The ureter above this section is dilated with reduced peristalsis because of relative obstruction (Meyer and Lebowitz 1992; Berrocal et al. 2002). The cause of the distal aperistaltic ureteral section is unclear, but may be related to excessive collagen deposition, ureteral muscle atrophy or hypertrophy causing a reduction or absence of peristalsis or innervation anomalies (Shokeir and Nijman 2000). The cause of non-refluxing unobstructed primary megaureter is also not clear. However, increased urine volume due to high glomerular filtration rate may be involved (Shokeir and Nijman 2000). Increased compliance of the ureter due to abnormal deposition of collagen, elastin or

Supported by the Veterinary Medical Teaching Hospital of Konkuk University, Republic of Korea.

doi: 10.17221/81/2017-VETMED

other proteins may affect the megaureter (Shokeir and Nijman 2000).

Congenital ureteral dilation associated with an ectopic ureter and secondary ureteral dilation is common in dogs (Steffey and Brockman 2004; Berent 2011). However, there are no reported cases of bilateral primary megaureter in which the distal ureteral segments exhibit no peristalsis and are of normal calibre. In addition, detailed ultrasonographic and computed tomographic features of primary megaureter have not been investigated in the veterinary field. This is the first known reported case of primary megaureter in a dog.

Case description

An 8-year-old male Alaskan malamute dog weighing 45 kg presented with symmetric alopecia, dyschesia, diarrhoea and undescended testes. The dog was previously prescribed antibiotics for the treatment of diarrhoea. There was no history of polyuria, pollakiuria, dysuria or oliguria. Findings on auscultation of the lungs and heart were normal. Abnormal laboratory findings were as follows: increased total protein (56 g/l; reference range, 26–40 g/l); neutrophilia (38 330/µl; reference range, 2950–11 640/µl); monocytosis (1710/µl; reference range, 160–1120/µl); eosinophilia (1320/µl; reference range, 60–1230/µl); increased serum oestradiol-17β (28.3 pg/ml; reference range, < 15 pg/ml); decreased testosterone (0.025 ng/ml; reference range, 0.288–5.760 ng/ml); and decreased testosterone/oestradiol ratio (0.0008; reference range, 0.0058–0.358). Serum blood urea nitrogen and creatinine levels were normal.

Lateral abdominal radiographs (Titan 2000M; Comed Medical Systems Co., Ltd., Seoul, Korea, 80 KVp, 300 mA) revealed tubular structures superimposed with bilateral kidneys, soft tissue opacities at the region dorsal to the urinary bladder and a large soft tissue opacity at the mid-ventral abdomen (Figure 1A). In addition, the radiographs revealed cranial displacement of the urinary bladder and the triangular region of fat between the craniоventral aspect of the prostate gland, caudoventral aspect of the bladder and ventral abdominal wall. The dimension of the prostate was 61% of the pelvic inlet dimension. Ventrodorsal radiographs (80 KVp, 300 mA) revealed a large soft tissue opacity in the right middle abdomen, which displaced the intestines cranially, caudally and left-laterally (Figure 1B). The left kidney/second lumbar vertebra (L2) and right kidney/L2 length ratios were 2.69 and 2.72, respectively.

Abdominal ultrasonography (US) revealed a large mass (approximately 66.6 × 57.9 × 74.4 mm) with unclear borders, heterogeneous echotexture and almost no vascular response in the region caudal and medial to the right kidney (Prosound Alpha 6, Aloka Co., Ltd., Tokyo, Japan, 4–13 MHz linear, 2.5–6.0 MHz convex and 3–9 MHz microconvex

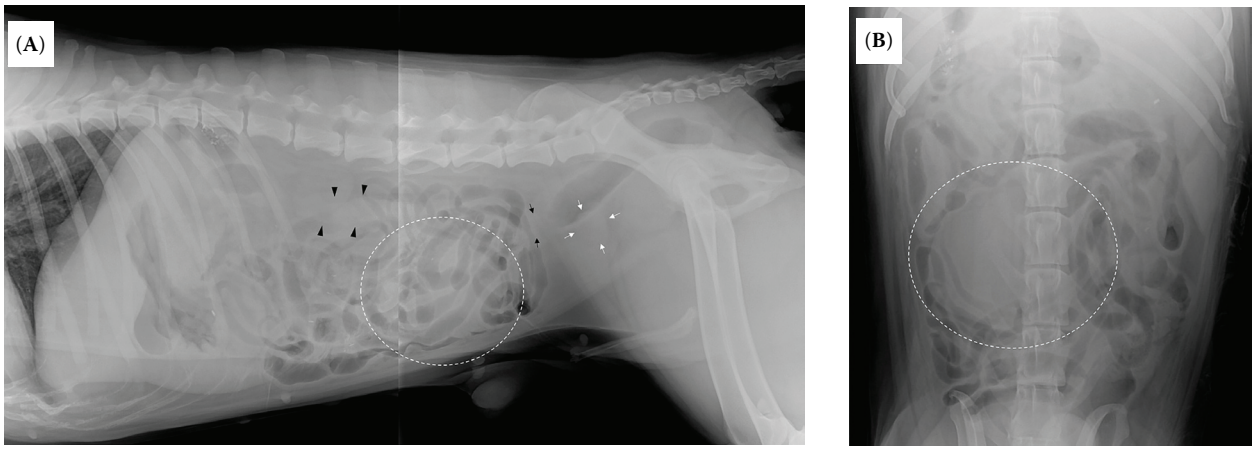

Figure 1. Right lateral and ventrodorsal radiographs. (**A**) A right lateral radiograph showing the tubular structure superimposed with bilateral kidneys (black arrowhead), a soft tissue opacity that bends the rectum towards the ventral direction at a region dorsal to the urinary bladder at the seventh lumbar vertebra level (black arrow), a soft tissue opacity between the rectum and the caudodorsal region of the urinary bladder (white arrow). In addition, a soft tissue opacity at the mid-ventral abdomen is identified (circle of broken line). (**B**) A ventrodorsal radiograph showing a soft tissue opacity that pushes the intestines in lateral, medial, cranial, and caudal directions (broken lined circle)

doi: 10.17221/81/2017-VETMED

transducers) (Figure 2A). In addition, an oval mass (approximately 14.2 × 7.3 × 6.2 mm) was identified in the region caudal to the left kidney. Tortuous vessels were detected in the region immediately caudal to each mass (Figure 2B). Mild dilation (approximately 2–3 mm) of the left and right renal pelvis was identified. In addition, both ureters were dilated (approximately 10–18.6 mm), and exhibited a tortuous course (Figures 2C, 2D and 2E) as well as reduced peristalsis. However, longitudinal US images of the distal ureteral segments about 10 mm from the vesicoureteral junctions revealed a normal calibre, aperistalsis and normal insertion into the urinary bladder (Figure 2F). Regardless of the differences in the sizes of the masses caudal to both kidneys, the dilation size of both ureters was the same and distal parts of the ureters not relative to the masses were also dilated, suggesting that the bilateral ureters were not compressed by the abdominal masses. The mucosal surface of the urinary bladder was mildly irregular, and the prostate was symmetrically enlarged (approximately 58.5 × 46.1 × 55.6 mm) with hypoechoic regions. Detection of ureteral jets with Colour Doppler could not be performed because of movements of the dog and artefacts. A urine sample was collected using cystocentesis. There was no evidence of abnormal findings on routine urine dipstick, specific gravity (1.03; reference range, 1.015–1.045), cytology and culture. Urine output evaluation by urethral catheterisation and urination pattern evaluation during cage rest was normal (92 ml/h; normal urine output, 2 ml/kg/h). Diagnoses of megaureter, intra-abdominal masses and prostatomegaly were made. The following temporary differential diagnoses were made based on the observed findings: primary and secondary megaureter for the megaureter; sustentacular cell tumour and seminoma due to cryptorchidism for the intra-abdominal masses; benign prostatic hyperplasia and prostatitis for the prostatomegaly.

Computed tomography (CT) and retrograde urethrocystography were recommended for the evaluation of the prostate, abdominal masses and

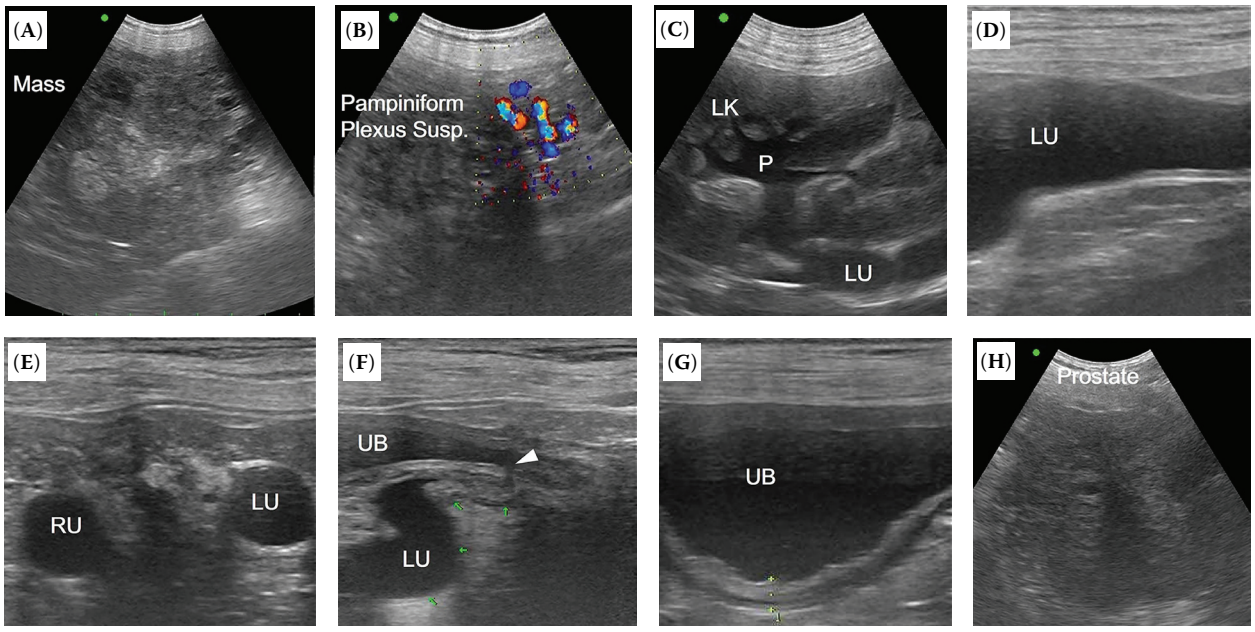

Figure 2. Ultrasonography images of the large mass and dilated ureters. (**A**) A large mass (approximately 66.6 × 57.9 × 74.4 mm) with heterogenous echotexture and unclear borders in the region caudal and medial to the right kidney. (**B**) The tortuous vessels were identified at a region caudal to the mass. (**C**) At the kidney level, a sagittal image shows dilation of the diverticuli (1–2 mm), pelvises (approximately 3 mm) and proximal ureters (approximately 9 mm). (**D**) Longitudinal image of the dilated proximal ureter. (**E**) Transverse image of the dilated middle ureter. The maximum diameter of the ureter was approximately 16 mm. (**F**) Longitudinal image of the left distal ureter segment 10 mm from the vesicoureteral junction showing a narrowed lumen and aperistalsis. The arrowhead indicates normal insertion of the left ureter. (**G**) Irregular mucosal surface of the urinary bladder with 4.1 mm thickness. (**H**) Enlarged prostate (approximately 58.5 × 46.1 × 55.6 mm) with hypoechoic regions

LK = left kidney; LU = left ureter; P = pelvis; RU = right ureter; UB = urinary bladder

doi: 10.17221/81/2017-VETMED

possible metastasis, as well as to visualise the detailed anatomic structure of the dilated and tortuous ureters and the presence of vesicoureteral reflux. However, the dog's owner requested only the removal of abdominal masses. The abdominal masses were removed surgically. After the surgery, medication including prophylactic antibiotics was administered to prevent urinary infections associated with the megaureter. The abdominal masses were diagnosed as a sustentacular cell tumour and seminoma due to intra-abdominal cryptorchidism on histopathological examination.

Sixteen days after the surgery, the owner consented to a CT scan to check for metastasis of the tumours, and to further evaluate the dilated and tortuous ureters. CT was performed for thorax and abdomen with a four multidetector-row system (LightSpeed; GE Medical Systems, Milwaukee) under isoflurane inhalation anaesthesia. The imaging parameters were as follows: 120 kVp, 200 mAs, 512 × 512 matrix, and 0.6 rotation time with a 2.5 mm slice thickness. Iohexol (Omnihexol 300; Korea United Pharmaceutical, Seoul, Republic of Korea) at 600 mg iodine/kg was injected manually

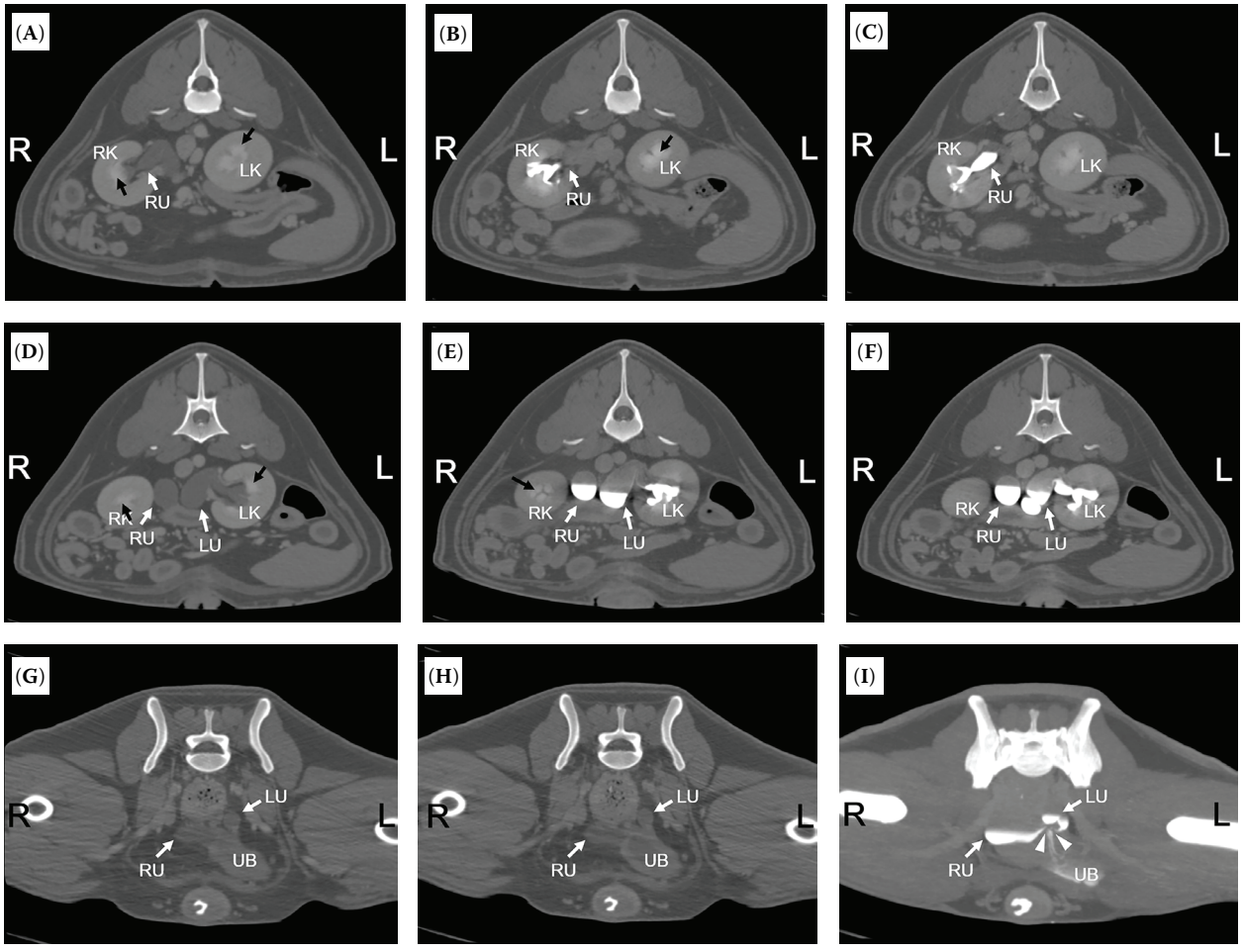

Figure 3. Computed tomography excretory urography images. Nephrogram 90 s ((**A**), (**B**) and (**G**)) and pyelogram and ureterogram 3 min ((**B**), (**E**) and (**H**)) and 7 min ((**C**), (**F**), and (**I**)) after injection of contrast medium. The images were obtained at the kidney level ((**A**), (**B**), (**C**), (**D**), (**E**) and (**F**)) and at the level of ureteral insertion into the urinary bladder ((**G**), (**H**) and (**I**)) with a window level of 300 and width of 1500. The black arrows indicate where the collecting system shows more contrast enhancement than the renal parenchyma. Two-dimensional images ((**B**), (**C**), (**E**) and (**F**)) show the dilated proximal ureters with a tortuous course and the inner contrast-urine level due to gravitation of the contrast medium. (**I**) The transverse maximum intensity projection images of 35 mm show bilateral ureteral jets in the urinary bladder indicating normal ureteral insertions. The white arrowheads indicate the left and right ureteral insertion regions with ureteral jets

LK = left kidney; LU = left ureter; RK = right kidney; RU = right urether; UB = urinary bladder

doi: 10.17221/81/2017-VETMED

into the cephalic vein. Contrast-enhanced CT images were acquired at 90 seconds, three minutes and eight minutes after the injection to evaluate renal function indirectly and to improve ureteral visualisation (Figure 3). All images were uploaded to free software (Osirix DICOM viewer; Pixmeo, Los Angeles) and reconstructed to images with a slice thickness of 1.25 mm to minimise stair-step artefacts during dorsal and sagittal reconstruction and three-dimensional volume rendering (Barrett and Keat 2004). The images were reviewed by two radiologists. Maximum intensity projection and three-dimensional volume-rendered images were obtained to improve the visualisation of both ureters.

In the CT excretory urography, the normal nephrogram phase was followed by a pyelogram and subsequent excretion of contrast into the ureters was observed. Bilateral ureter dilation with a tortuous course was also visible (Figure 3 and Figure 4). Gravitation of the contrast medium and a contrast-urine level was seen in the images because specific gravity differed between the contrast medium and the urine. The tortuous ureteral course from the distal ureter to the urinary bladder was therefore difficult to appreciate on the two-dimensional transverse CT images, but was easily visible, together with the insertion and ureteral jets, on the maximum intensity projection and three-dimensional volume-rendered images (Figure 3I and Figures 4D and 4E). Nevertheless, the maximum intensity projection and three-dimensional volume-rendered images could not completely reveal the ureteral courses because the ureters were not completely filled with contrast medium (Figure 4). The enlarged prostate with multiple non-enhanced regions was identified on post-contrast images. Metastasis of the sustentacular cell tumours and seminoma was not detected on thoracic and abdominal CT.

At the two-month follow-up, the dog showed no symptoms related to the urinary system. Mildly dilated renal pelvises, dilated and tortuous ureters with reduced peristalsis and distal ureteral

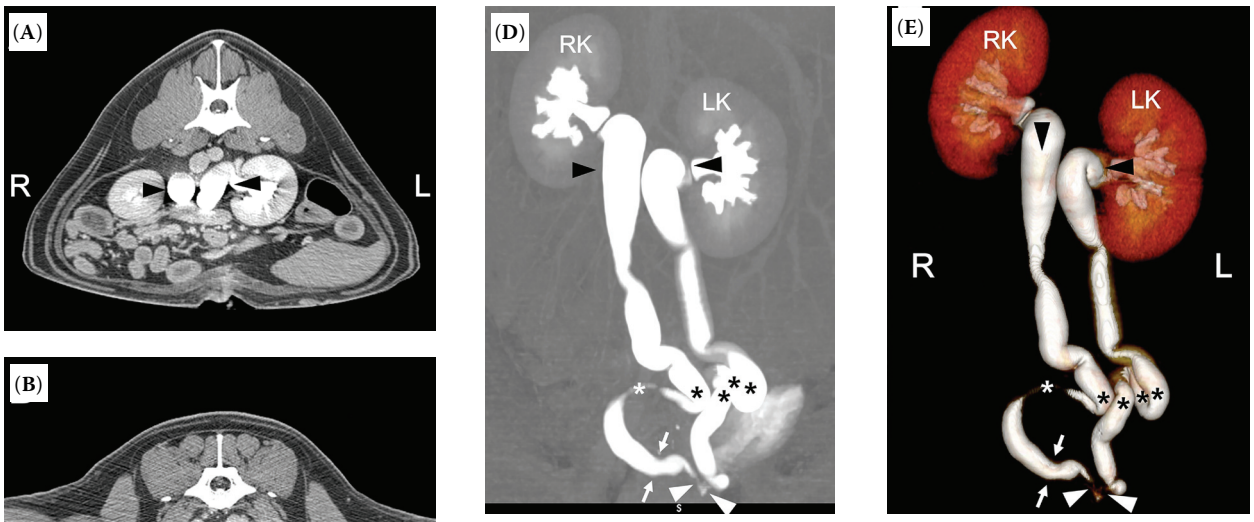

Figure 4. Two-dimensional computed tomography, maximum intensity projection, three-dimensional volume-rendered images of bilateral kidneys and ureters. The two-dimensional transverse images show the dilated proximal ureters (black arrow heads) (**A**), severely tortuous travels of the ureters (asterisks) (**B**) and the right distal ureter (white arrows) that runs transversely, wandering laterally (**C**). Dorsal images of maximum intensity projection (67 mm thickness) (**D**) and three-dimensional volume rendering (**E**) show the complicated and tortuous course of the bilaterally dilated ureters (asterisks)

Black arrowheads, asterisks and white arrowheads indicate the regions that could be superimposed and could cause increased soft tissue opacity on the lateral radiograph. The white asterisk indicates the right ureter that is not filled with contrast medium. The white arrowheads indicate ureteral insertion points. Re = rectum; RK = right kidney; LK = left kidney

doi: 10.17221/81/2017-VETMED

segments with aperistalsis were still identified on ultrasonography, similar to the previous findings. The size of the prostate was reduced (37.9 × 29 × 37.8 mm) and the hypoechoic regions had disappeared. Alopecia improved as well.

A diagnosis of primary megaureter was made for the ureters based on the lack of evidence for congenital anomalies or obstructive problems of the urethra and urinary bladder on radiographic, ultrasonographic and computed tomographic examinations, and based on the lack of clinical findings for urine output and urination pattern (Shokeir and Nijman 2000). Prophylactic antibiotics were continuously prescribed to prevent secondary infections due to prolonged urinary emptying time in the megaureters (Gimpel et al. 2010).

DISCUSSION AND CONCLUSIONS

Primary megaureter in humans can be diagnosed early by foetal ultrasound, but if it does not result in specific symptoms, its diagnosis may be delayed due to late referral to a hospital (Shokeir and Nijman 2000). In this case, the 8-year-old Malamute did not exhibit any special clinical symptoms associated with the urinary system. Therefore, megaureter of animals without clinical signs affecting the urinary system may be identified only at a late age.

In the present case, US examination made it possible to identify the aperistaltic distal ureteral region with normal ureteral calibre and insertion into the urinary bladder and the peristaltic ureter above the region, which are features of the obstructed primary megaureter (Berrocal et al. 2002). CT excretory urography made it possible to evaluate complicated ureteral courses definitively and to indirectly probe renal function. However, the delayed drainage of urine due to increased ureteral compliance resulted in gravitation of the contrast medium, and consequently, generation of a contrast-urine level in the images. A further reduction in peristalsis due to isoflurane inhalation anaesthesia may have caused the phenomenon (Young et al. 1994). It is worth noting that these problems related to incomplete opacification in dilated ureters may also appear on radiographic excretory urography (Cohan and Caoili 2007).

This case was difficult to diagnose with primary megaureter at the first visit because of cystitis. It is possible that the ureter was dilated by infection, but ureteral dilation can also cause urinary infection (Gimpel et al. 2010). However, the cystitis was mild; infectious agents were not identified; specific problems of renal function related to urinary obstruction were not identified; the dilation of the renal pelvises was mild; and there were no clinical signs related to obstruction of the lower urinary tract, such as anuria or oliguria. Therefore, we made a diagnosis of primary megaureter.

Identification of primary megaureter subtype was difficult in this study. In humans, if secondary causes of megaureter are excluded, retrograde cystourethrography or echo-enhanced cystosonography can be attempted for differentiation of vesicoureteral reflux (Shokeir and Nijman 2000; Berrocal et al. 2001). Subsequently, radionuclide renography is performed to evaluate renal function and obstruction (Shokeir and Nijman 2000). Although there are no gold standard procedures for differentiating obstructed and non-obstructed megaureter, renography may be helpful in the differentiation (Shokeir and Nijman 2000). However, renography is not a widely used diagnostic method in veterinary medicine, and ultrasonography may, therefore, be more useful. On ultrasonography, the presence of obstructed primary megaureter may be suggested by normal calibre and aperistalsis of the short distal ureter connected to the vesicoureteral junction, and dilated ureter with reduced peristalsis above this short distal ureter (Meyer and Lebowitz 1992; Berrocal et al. 2002).

The surgical correction of megaureters to preserve normal renal function is controversial. However, high-grade vesicoureteral reflux decreases renal function due to obstruction. Moreover, renal infection may necessitate surgical correction including ureteral plication, bypass surgery or distal ureter resection and remodelling (Shokeir and Nijman 2000). Prophylactic antibiotics are strongly recommended for megaureter and may prevent ascending renal infection, sequential renal failure and systemic infection (Shokeir and Nijman 2000; Berrocal et al. 2002).

Retrograde cystourethrography, echo-enhanced cystosonography, radionuclide cystography and radionuclide renography were not performed in the scope of this work and this represents a drawback of the current study. The normal calibre of the distal segments of both ureters may indicate that obstructed primary megaureter was much more probable in this case than non-obstructed primary

doi: 10.17221/81/2017-VETMED

megaureter (Meyer and Lebowitz 1992). However, the normal ureteral jets and nephrogram with mild dilation of bilateral renal pelvises on CT excretory urography might indicate the presence of mild obstruction. The possible concurrence of obstructed primary megaureter, vesicoureteral reflux and abnormalities of the ureteral tissue matrix cannot be completely excluded.

In conclusion, this case report is the first to describe ultrasonographic and computed tomographic features of primary megaureter in a senior Alaskan malamute dog. A differential diagnosis of primary megaureter should be included in dogs with a dilated ureter that is not caused by obstructive diseases of the urinary bladder or urethra. A combination of ultrasonographic, two-dimensional computed tomographic, maximum intensity projection and three-dimensional volume rendering modalities can be useful in the diagnosis of primary megaureter and in the detailed visualisation of clinical features.

REFERENCES

Barrett FB, Keat N (2004): Artifacts in CT: recognition and avoidance. Radiographics 24, 1679–1691.

Berent AC (2011): Ureteral obstructions in dogs and cats: A review of traditional and new interventional diagnostic and therapeutic options. Journal of Veterinary Emergency and Critical Care 21, 86–103.

Berrocal T, Gaya F, Arjonilla A, Lonergan GJ (2001): Vesicoureteral reflux: Diagnosis and grading with echo-enhanced cystosonography versus voiding cystourethrography. Radiology 221, 359–365.

Berrocal T, Lopez-Pereira P, Arjonilla A, Gutierrez J (2002): Anomalies of the distal ureter, bladder, and urethra in children: Embryologic, radiologic, and pathologic features. Radiographics 22, 1139–1164.

Cohan RH, Caoili EM (2007): CT urography techniques. In: Silverman SG, Cohan RH (eds): CT Urography: an Atlas. 1st edn. Lippincott Williams and Wilkins, Philadelphia. 15–17.

Gimpel C, Masioniene L, Djakovic N, Schenk JP, Haberkorn U, Tonshoff B, Schaefer F (2010): Complications and long-term outcome of primary obstructive megaureter in childhood. Pediatric Nephrology 25, 1679–1686.

Gross GW, Lebowitz RL (1981): Infection does not cause reflux. American Journal of Roentgenology 137, 929–932.

Kass EJ (1992): Megaureter. In: Kelalis PP, King LR, Belman AB (eds): Clinical Pediatric Urology. 3rd edn. Saunders, Philadelphia. 781–821.

Khoury A, Bagli DJ (2007): Reflux and megaureter. In: Wein AJ, Kavoussi LR, Novick AC, Partin AW, Peters CA (eds): Campbell-Walsh Urology. 9th edn. Elsevier Inc, Philadelphia. 3467–3468.

Meyer J, Lebowitz R (1992): Primary megaureter in infants and children: A review. Urologic Radiology 14, 296–305.

Shokeir AA, Nijman RJM (2000): Primary megaureter: Current trends in diagnosis and treatment. BJU International 86, 861–868.

Smith ED, Cussen LJ, Glenn J (1977): Report of working party to establish an international nomenclature for the large ureter. Birth Defects Original Articles Series 13, 3–8.

Steffey MA, Brockman DJ (2004): Congenital ectopic ureters in a continent male dog and cat. Journal of the American Veterinary Medical Association 224, 1607–1610.

Young CJ, Attele A, Toledano A, Nunez R, Moss J (1994): Volatile anesthetics decrease peristalsis in the guinea pig ureter. Anesthesiology 81, 452–458.

Received: June 13, 2017
Accepted after corrections: December 15, 2017